Progress In Electromagnetics Research, Vol. 110, 43–58, 2010

SENSOR AREA NETWORK FOR ACTIVE RTLS IN RFID TRACKING APPLICATIONS AT 2.4 GHZ

A. V. Alejos, M. G. Sanchez, I. Cuiñas and J. C. G. Valladares

Department of Teoria de la Señal y Comunicaciones
University of Vigo, Campus Universitario Lagoas, Vigo 36310, Spain

Abstract—Power strength or Received Signal Strength Indicator (RSSI), a primary technique used in Real Time Location Systems (RTLS), is analyzed in this paper for RFID tracking applications. Critical issues are studied and hardware novelties are introduced in order to improve its performance. The main novelty is the accomplishment of an RFID RTLS through a mesh of individual active radiofrequency (RF) barriers composed by active emitter and receiver nodes/tags that cover only small individual areas. The result is a Sensor Area Network (SAN) that offers some advantages over classical tracking systems, which are based on Wireless Sensor Networks (WSN), especially in the multipath impairment mitigation, such as a controlled power emission, and the chance to warrant privacy regarding the exchange of RFID information. Experimental measurements were done to estimate the influence of the transmitted signal type and the receiver end architecture in the detection of the RF barrier presence. The parameterization of the coverage area of a SAN cell in terms of power is derived for both free-space and log-distance propagation models. The Kalman filtering technique is introduced as a valid tool to severely mitigate the multipath propagation effects that can affect the accurate operation of the proposed SAN for indoor operation conditions. Outcomes show a promising performance for this wireless network design, which has not received enough attention in literature.

1. INTRODUCTION

Many systems and applications need the benefits derived from the use of location techniques that complement their capabilities and

Received 2 October 2010, Accepted 29 October 2010, Scheduled 8 November 2010
Corresponding author: Ana Vazquez Alejos (analejos@uvigo.es).

also improve their offered features [1–5]. One of those is the Radio Frequency Identification Device (RFID) technology. In this paper, the use of Real Time Location Systems (RTLS) is considered as a component and not only as a value added. The addition of location techniques to the RFID technology can contribute to reduce the packet data loss; thus, the traceability of the objects/tags movement is facilitated, which minimizes the request rate of the reading network.

Among others, three major techniques can be selected to implement a RTLS [6–10]: according to the estimation of the received signal strength or RSSI (Received Signal Strength Indicator); according to the direction finding theory, such as the estimation of the Angle of Arrival (AoA), or Time of Arrival (ToA/TDoA), or well a combination of them; and finally, using wideband technologies that involve the use of spreading codes.

The main benefits and disadvantages of these location techniques are well-known and multiple methods have tried to solve them. Perhaps the simplest location technique is the one based on the Received Signal Strength Indicator (RSSI) estimation [11–16]. Despite its associated problems, mostly due to the multipath influence on the provided accuracy, it constitutes a cost affordable technology, which is perfectly suitable for simple tracking applications as long as that line-of-sight (LOS) condition can be ensured.

By means of the training or footprint recognition technique, the RSSI location systems can improve their location capacities. Alongside with these methods, we propose a system named Sensor Area Network (SAN) as a RFID RTLS formed by a mesh of individual radio frequency barriers, each of which is limited to a restricted operation area.

This type of system has found scarce attention in the literature [17–19]; notwithstanding, it can offer some important advantages over the classical tracking technologies based on WSNs implementing ZigBee (IEEE 802.15) or WiFi (IEEE 802.11x) standards. In the latter, the possibilities of achieving large accuracy rates in the location estimation are reduced due to several factors or impairments mostly caused by the intrinsic features of these networks [17]: the transmission in wireless network access points (APs) is not continuous, which makes obtaining a good signal strength triangulation difficult even if averaging is applied; the wireless network AP data rate is variable depending on the number of connected users; the "noise" present in the channel cannot be neglected and is caused by a large number of asset RFID tags, regular users of the WiFi as a communication system, and other interfering systems that can freely operate in the 2.4 GHz band; the large number of APs needed to ensure a location with equal accuracy to that of a room can

compromise the accomplishment of emission regulations especially in sensitive scenarios.

Tracking systems based on *ad-hoc* designs can offer larger accuracy levels than WiFi-based solutions, but they also present important disadvantages, which, on many occasions, are related to the system modularity and the difficult maintenance and calibration. In this paper we present one of these specific tracking systems, the SAN, as a cost affordable and reliable alternative to classical WiFi-based tracking systems. The technique here introduced presents a double potential: acting as an RTLS for RFID tracking applications, but also as a WSN.

A SAN is composed of a mesh of individual sensors or reader nodes placed in specific and strategic spatial positions; those sensors or reader nodes can register the user moving tags as they come in and out of their operation zone or coverage area. The coverage area is divided in single nodes or cells that can follow the movement of the user tags. The capabilities (transmitter/receiver/transceiver) of each element (cell node/moving tag) have to be defined a priori.

For intended use in RFID tracking, this operation principle offers one important additional option to warrant the privacy of the tags. If the detection capacity for the SAN nodes drops on the active moving tags, a tagged asset penetrating a cell can decide if it reveals its presence in the network. Actually, any generic RFID reading network may implement this node detection capability as a complementary tool to identify specific tags or reader nodes, and as a way to estimate the movement direction of tag subsets.

For a SAN system, the propagation phenomena can limit the provided benefits and, thus, constrain the reliability of signal strength estimation. Attenuation and signal fading, time dispersion and frequency fading caused by the multipath propagation or by people moving in the surroundings of reader terminals/nodes/tags, are undesired impairments, sometimes characterized by time-varying features, which make the compensation of the associated effects extremely difficult. This is a key problem because the success of tracking systems based on RSSI estimation depends on its ability to keep a received signal power similar to LOS conditions despite the impairments produced by the propagation channel. The receiver front-end sensitivity largely constraints the capacity of a user moving tag to detect the coverage areas, namely cells.

In this research work, we analyze and discuss the influence of four hardware architectures to accomplish the node detection capability in the ISM unlicensed frequency band of 2.4 GHz. They have been analyzed in combination with two options for the transmitted signal: continuous wave (CW) or modulated wave. In this scenario, the

Kalman filtering technique can be applied to mitigate the propagation impairments resulting in improvement of the node/tag detection capability by increasing the signal strength estimation accuracy. We can find in the literature a good number of algorithms that include the performance of a Kalman filter, as well as the extended Kalman filters (EKF) version. Many of them have been applied to location estimation applications with good results either on WiFi or Zigbee (IEEE 802.15) based systems [20, 21].

In our work, we have deployed one single SAN cell with a detection capacity relegated to the moving tag. Experimental measurements have been conducted in actual scenarios showing a good accuracy in the position estimation, as well as an adequate robustness against interferences produced by neighbour *WiFi* networks and multipath impairments. Different transmitted signals have been tested, some of them proposed for the RFID standard [22], in combination with the examined receiver front-end architectures.

In Section 2, we extend the concept of SAN systems, examining some critical issues of this tracking technology, and we discuss its practical implementation. In Section 3, we evaluate the influence of the transmitted-signal/receive-end-technology pair on the cell node detection accuracy. The outcomes of the conducted experimental measurements are commented in subsection 3.3. In Section 4, we present the Kalman filtering as a valid tool to mitigate multipath impairments, which affect a SAN-based tracking system for real time operation conditions. Finally, the conclusions offered in Section 5 close this paper.

2. SENSOR AREA NETWORKS

The SAN system considered for this study constitutes a mesh of individual RF barriers, each of which works according to the same principle of a laser barrier. The main advantage of the radio version of a barrier is the robustness against the environmental conditions, such as dust, particles in the air or humidity. Basically, an RF barrier consists of a transmitter that sends information, modulated or not, and a receiver that can detect and measure some parameters of that signal in order to detect the barrier presence. Actually, both ends of the barrier can present additional capabilities, as transceivers that decide to act in a barrier mode under specific circumstances.

If the parameter selected to estimate the presence of a barrier is the signal amplitude, the range or spatial limits of the RF barrier or cell are given by a limit value that must be determined in accordance with the sensibility of the receiver architecture. If the parameter level

measured by the tag is greater than the delimiting value, the tag can consider itself located within the area delimited by the RF barrier. This happens under ideal propagation conditions: if the multipath and the interferences do not cause important impairments in the travelling signal.

Although the physical perimeter of the RF barrier is delimited in terms of signal parameters, the shape of the coverage area depends on the antenna pattern footprint, but it can be basically considered circular or ellipsoidal. This consideration will be taken into account when dimensioning the cell range.

The operating principle of the SAN system will be as follows: a tag (moving user) will send information required from a reader (static cell node) while it stays within a restricted area. Besides, the tag can also be equipped with an additional feature. As an RFID system that can preserve the privacy of the tag, the tag knows that it is placed in a specific region, and, then, decides if a transmission must be performed or not, independently of the query performed by the reader; that constitutes an intelligent choice. This last performance would require an active tag, a smart location algorithm and some additional hardware on the tagged asset.

The hardware architecture to be implemented in the receiver end of a moving tag in order to detect the RF barrier presence will depend firstly on whether the transmitted signal is modulated or not. Basically, in this scene, the main options for a receiver end consist in a heterodyne front-end, a power detector and an envelope detector. We have also added one more alternative given by a heterodyne receiver provided with an envelope detector at the non-zero Intermediate Frequency (IF) output.

In the next section, the combinations resulting from the transmitted signal type and the receiver end architecture options have been used to determine the coverage area provided by an RF barrier and the accuracy reached by each combination in the detection of the barrier presence. This detection has been fixed in terms of measured radio range. If we choose the power level as signal parameter to monitor, it can be translated into a receiving distance value or radio range. According to the transmitted power and the budget link, the theoretical radio range can be compared with the measured range. From this comparison the decision on the cell presence is taken.

The following expression (1) has been applied to obtain the theoretical coverage area or radio range, assumed as a circular shape zone of radio r in meters:

$$r \leq \sqrt{10^{(P_{Tx}+G_{Tx}+G_{Rx}-32.4-20\cdot\log_{10} f-S)/10} - h^2} \tag{1}$$

The above range parameterization was derived taking into account

the condition to determine the limit of the barrier in terms of power (2), the free-space propagation model (3) and the cell geometry setup described in Figure 1:

$$P_{Rx} \leq S \tag{2}$$

$$P_{Rx} = P_{Tx} + G_{Tx} + G_{Rx} - 32.4 - 20 \cdot \log_{10} f - 20 \cdot \log_{10} d \tag{3}$$

where P_{Tx} is the power of the transmitted carrier in dBm; G_{Tx} and G_{Rx} are the transmitting and receiving antenna gain in dBi; f is the frequency expressed in GHz; h is the transmitter antenna height in meters; and S is the receiver sensitivity in dBm. The graphical illustration of the geometry assumed for the RF barrier is shown in Figure 1. The possibility of using antennas with no isotropic radiation patterns, and even with mechanical or electronic tilt degree β, can be considered.

A fit using a log-distance model ($P_{Rx} = P_0 - 10n \log_{10} x$) was discarded after finding that the power-decay factor n was around 2, as found in free-space conditions. This model should be considered for other values of n, and so the range r (1) would be expressed as in (4):

$$r \leq \sqrt{10^{2(P_0 - S)/10n} - h^2} \tag{4}$$

where P_0 should be estimated for a reference point within the coverage area, and would include the transmitter and receiver antenna gains. The coverage area is assumed to be illuminated by the main antenna

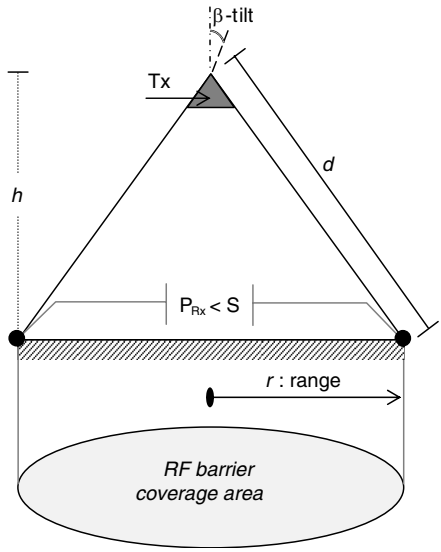

Figure 1. Geometry of a SAN cell.

lobe, within the region of the 3 dB beam width; under that condition, antenna gains can be considered as constant. For any other case, a correction factor must be included. Another equally important aspect to consider is the depolarization of the antennas that can be easily incorporated in (1) and (4) as a loss factor.

3. EXPERIMENTAL MEASUREMENTS

Two kinds of transmitted signals have been tested. In the unmodulated case, a CW single carrier is transmitted at 2.45 GHz; in the second case, a GMSK modulation is applied. In the latter, the modulation will help to mitigate part of the interferences in the largely radio-electrically polluted 2.4 GHz ISM band. The modulated transmission option is aligned to the standard developed for RFID systems working in this frequency band [22].

During all the experimental measurements, the transmitter end consisted of a generator and an isotropic antenna placed at the room ceiling at a height h of 3 m. The power of the transmitted signal was changed according to the receiver scheme used. The transmitter set-up has been depicted in Figure 2.

Measurements have been carried out in an open area inside an actual room, free of furniture, and under quiescent conditions. Some of the few elements of the scenario, such as the ceramic floor, are supposed to present large reflection coefficients. Regardless of this fact, distortions did not seem to affect the registered signal.

We delimited the maximum measured range area by finding the point in which the received power stopped being greater than the noise, which prevented distinguishing both signals. This point is called the barrier limit. The received power measurements were performed along two perpendicular diameters of a 9 m-radius circumference, which was centered in the transmitting antenna placement; those measurements were taken in every meter of the diameter at ground level.

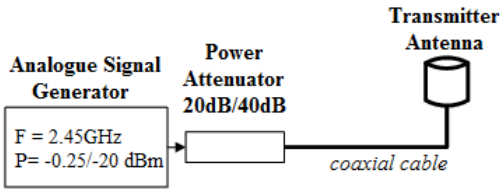

Figure 2. Diagram block for CW transmission end.

Table 1. Receiver architectures and delimiting ratio for RF barrier and other parameters.

Transmission & Transmitted Power P_{Tx}		Receiver architecture	Sensitivity S (dBm)	Measurement procedure	Range r (m)	Delimiting Ratio = $P_{Rx\,out} / P_{Rx\,in}$
CW (Section 3.1)	CW @ -40.25dBm	Heterodine front-end	-100	Peak Power level	9	-90 / -100
	CW@ -40.25dBm	RMS power meter	-100	RSSI	8	-83 / -89
	CW@ -20.25dBm	Heterodine front-end & Envelope Detector	-35	Peak voltage level	9	-19 / -31
Modulated (Section 3.2)	GMSK @ -0.25dBm	RMS power meter & Envelope Detector	-100	RSSI	7	-52 / -62

In the following subsections 3.1 and 3.2 we describe the different receiver schemes implemented for each kind of transmitted signal described below. In Table 1, we summarize the combinations detailed in subsections 3.1 and 3.2 in terms of the main parameters of the experiment performed, such as transmitted power P_{Tx} and receiver sensitivity S. Later in 3.3, we present the results obtained from the actual measurements with the described combinations.

3.1. Single Carrier CW Transmission

A CW transmission is applied to send a single carrier at 2.45 GHz. The first receiver scheme used is based on a spectrum analyzer. In this case, the signal received by a stub omnidirectional antenna is visualized in a spectrum analyzer configured to determine the peak power level of the received carrier using the RMS detector. In this configuration the spectrum analyzer is equivalent to a heterodyne receiver. The sensitivity of this configuration is -100 dBm.

The second tested receiver consisted of measuring the power of the signal on a supposed 500 kHz bandwidth channel. The channel power measurement option given by the spectrum analyzer was employed. In this configuration the spectrum acts as an RMS power meter. The sensitivity was -100 dBm.

The third receiver architecture used consisted of an ad-hoc receiver as shown in Figure 3. We used a heterodyne receiver with output at an IF of 70 MHz. This IF was applied to an envelope detector and the peak amplitude of the voltage signal present at its output was measured by an oscilloscope. The sensitivity of this receiver architecture, -35 dBm, is given by the detector. In this third case, the power of the transmitted carrier was increased from -20.25 dBm to -0.25 dBm to compensate the lower value of sensitivity achieved by this receiver scheme.

3.2. Modulated Transmission

A GMSK signal was transmitted with a centre frequency of 2.45 GHz. The data rate selected was 250 Kbps, with a Gaussian filter of bandwidth-time product $0.3\,B \cdot T$, where B is the used bandwidth for transmission and T the selected bit pulse. The product $B \cdot T$ is related to the filter -3 dB bandwidth and data rate by $BT = -3$ dB-cutoff-frequency/data-rate. The bandwidth of the transmitted signal is 2 MHz. An advantage of this case is the double functionality offered as a RF barrier and a wireless information system. A block diagram of this GMSK transmitter can be seen in Figure 4. The transmitter version for a SMA connectorized antenna can be observed in Figure 5.

The receiver scheme considered for the modulated transmission case consisted of the combination of a superheterodyne downconverter and an envelope detector. The signal was captured by an omnidirectional stub antenna, amplified and later on downloaded by a mixer to an IF of 70 MHz. This IF signal was amplified again and bandpass filtered before being driven to an envelope detector. The voltage amplitude signal offered by the Schottky diode detector was

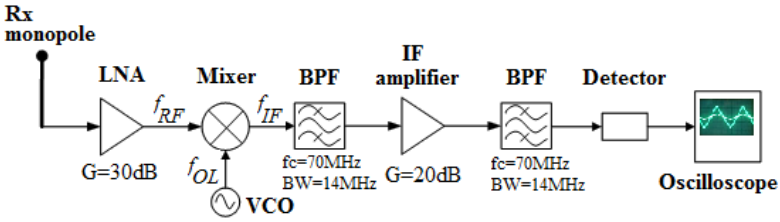

Figure 3. Diagram block for super-heterodyne receiver end with envelope detector.

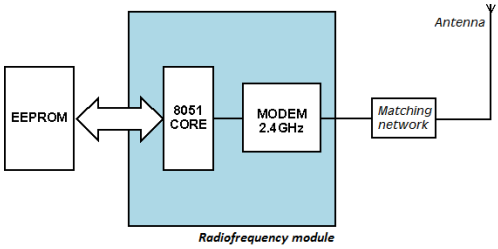

Figure 4. Diagram block for the GMSK transmitter.

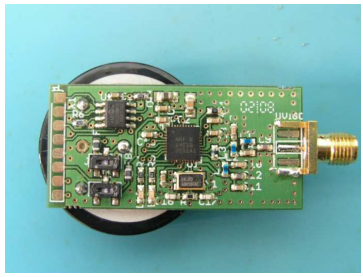

Figure 5. SMA connectorized antenna implementation of GMSK transmitter.

observed in an oscilloscope and its RMS value was calculated. This scheme based in an envelope detector corresponds with many actual systems. The block diagram is the same as shown in Figure 3.

The sensitivity value of the Schottky detector is −35 dBm, as indicated above; thus, a transmitted power of −0.25 dBm was used again.

3.3. Experimental Results

In the four front-end cases, the analysis performed consisted of determining the range obtained through practical power measurements. The power levels of the signals observed at the output of each receiver scheme have been compared with the ideal value given by the free space model as plotted in Figure 6. In Table 1 the range achieved for the different cases are summarized. For the first and second receiver cases, the theoretical and the measured radio ranges are very close. In the other two cases, we observe a measured range inferior to the theoretical one of 9 m.

However, this comparison, according the measured range, does not seem to be enough to determine the goodness of a receiver hardware scheme. This fact drives us to define a new parameter in order to estimate the accuracy in the estimation of the RF barrier limit. Additionally, the power of the transmitted signal differs from one end-architecture to another, then we have defined a new parameter in order

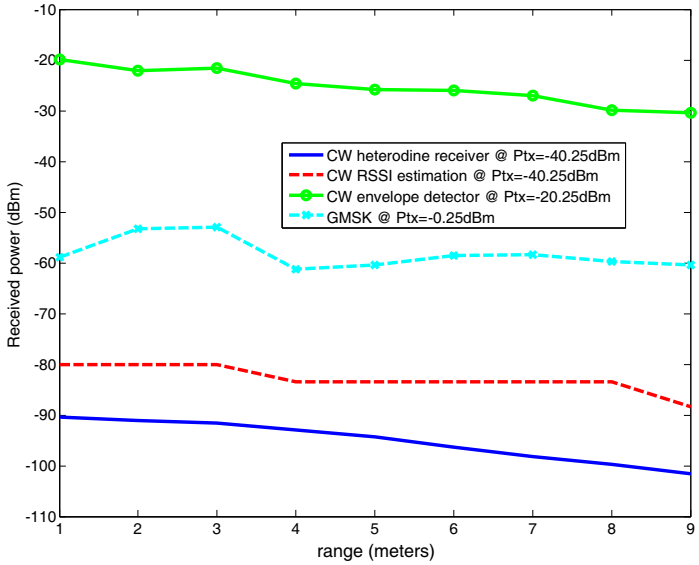

Figure 6. Comparison of measured ranges.

to achieve a more meaningful comparison of the different architectures' behavior. This parameter takes into account the power level measured inside the area delimited by the barrier and the power found outside the limits. We have named this parameter Delimiting Ratio (DR) and it is given by the ratio of the averaged highest power measured within the barrier and the noise power level measured in the barrier limit. This parameter constitutes a measurement of the receiver accuracy to determine the presence of the RF barrier.

In Table 1, we also summarize the values of the DR parameter obtained for the different receiver architectures considered. A larger value of DR indicates that the system has larger reliability to detect the barrier and a more optimal robustness against interferences and multipath. According to this criterion, the combination of a CW single carrier and a receiver architecture formed by a heterodyne receiver and an envelope detector seems to be a suitable candidate for a practical implementation of a SAN-tag; however, this scheme presents a disadvantage due to the limited range detection of the envelope detector, which requires a larger transmitted power.

4. KALMAN FILTERING

The selected discrete Kalman filter has been defined for a state space model given by Eq. (5) that evaluates the actual state as a function of the last state (Δr space units before).

$$X_k = A \cdot X_{t-\Delta t} + B \cdot u + w = A \cdot X_{k-1} + B \cdot u + r \tag{5}$$

$$A = \begin{pmatrix} 1 & \Delta r \\ 0 & 1 \end{pmatrix} \quad B = \begin{pmatrix} 1 \\ 0 \end{pmatrix} \tag{6}$$

In (5), the present state of the system is defined by the two components: vector X_k, which contains the present RSSI measurement of the tracking object, and the distance increment, Δr. That yields to the measurement equation as follows:

$$X_k = \begin{pmatrix} \text{RSSI} \\ \Delta r \end{pmatrix} \cdot X_{k-1} + q \tag{7}$$

The Δr space difference between consecutive samples $(k, k+1)$ was set to 0.1 m. The measurement model will consider both the noise process covariance matrix Q and the measurement noise covariance matrix R as white Gaussian and additive processes:

$$Q = \begin{pmatrix} q & 0 \\ 0 & q \end{pmatrix} \tag{8}$$

$$R = \begin{pmatrix} 0.03 & 1 \\ 1 & 0.03 \end{pmatrix} \tag{9}$$

In (8), q is the variance of the white Gaussian noise that perturbs the measure, and has been fixed to 0.1 in our example; and r is the variance of the noise found in the measurement process. The actual power strength $X_k = (\mathrm{RSSI}_{\mathrm{meas}}, r_{\mathrm{meas}})$ is given by the previous position estimation algorithm of (7), X_{k-1}, where X_0 is the initial state given by (10):

$$X_0 = \begin{pmatrix} \epsilon & 0 \\ 0 & \epsilon \end{pmatrix} \tag{10}$$

Here ϵ is the initial error of the first position estimation. In our case, this value was set to 0.1 m. The estimated filtered value is given by following this formulation, according to [20, 21]. Finally, the Kalman gain is K and the matrix H is given by (11):

$$H = \begin{pmatrix} 1 & 0 & 0 & 0 \\ 0 & 1 & 0 & 0 \end{pmatrix} \tag{11}$$

The Kalman filter has been applied to the GMSK transmission combined with RSSI estimation case. Measurements were performed in the same actual scenario as described in Section 3. We followed the 9 m-diameter radius, but forced the presence of large multipath through people moving around the receiver. We have established a relation between the RSSI and the radio of the coverage area according to the measurements described in subsection 3.3 to determine the DR factor. The relation distance-RSSI approaches a slope $-10\,\mathrm{dBm}/7\,\mathrm{m}$.

The Kalman filter offers an estimate position, inside the coverage area, using previous values of RSSI and according to the space variation, from the centre (maximum RSSI) towards the edge (minimum RSSI). The estimated position values are plotted jointly with the theoretical curve — given by a free space propagation model with slope $-1.428\,\mathrm{dBm/m}$, and also with the actual positions resulting from the measured RSSI values. This comparison can be observed in Figure 7. In Table 2 we provide the discrete values of the three plotted curves to facilitate the comparison.

We can notice that the measured values differ from the theoretical ones the closer to the edge of the coverage area. The error in the estimation of the position reaches up to 3 m, but the Kalman filter reduces it drastically. Whilst the median error presented by the actual measurements regarding the theoretical values is of 2.173 m with a standard deviation of 2.24 m, the values predicted by the Kalman filter shows a mean error of 0.528 m with a standard deviation of 0.9 m. We can check that the Kalman filtering is a good technique to reduce the multipath impairments for a SAN system improving the node detection accuracy.

Table 2. Dicrete values of curves plotted in Figure 7.

RSSI (dBm)		-52	-52.7	-53.4	-54.1	-54.8	-55.5	-56.2	-56.9	-57.6	-58.3	-59	-59.7	-60.4	-61.1	-61.8	-62.5	-63.2
Position (m)	Theoretical	0.09	0.45	0.91	1.36	1.81	2.27	2.72	3.18	3.63	4.09	4.54	5	5.45	5.91	6.36	6.82	7.27
	Measured	0.1	-0.06	0.79	1.65	2.34	2.19	3.72	4.11	4.19	5.03	4.91	5.84	6.01	4.97	6.42	6.51	7.22
	Kalman corrected	-0.16	-0.07	0.79	1.79	3.35	3.75	5.22	6.07	6.56	6.89	7.20	8.38	7.69	8.14	9.19	9.31	10.55

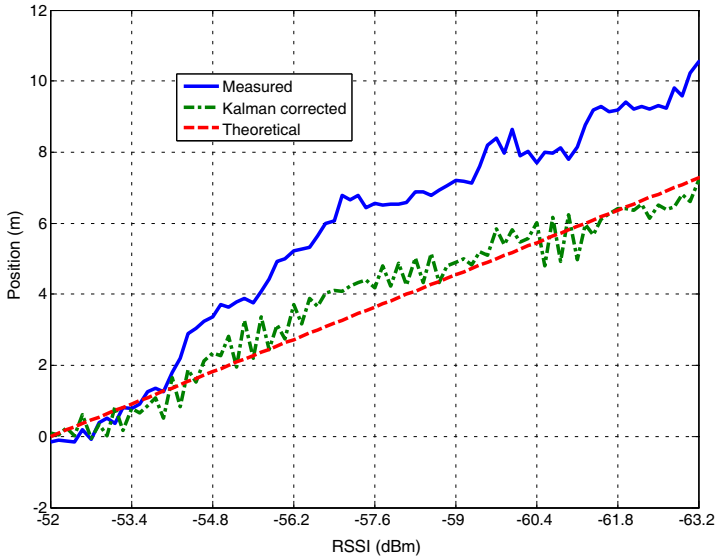

Figure 7. Position estimation by Kalman filtering.

5. CONCLUSIONS

Generally speaking, we observe that the results obtained for this experiment show good potential for a simple and low-cost RTLS oriented to a RFID tracking application based on a SAN system. This type of network consists of a mesh of interconnected RF barriers. In spite of the important benefits in location applications, mostly if privacy is required, and the results it has provided, few references can be found in the literature.

In this paper, the influence of the receiver end architecture on the accuracy to detect the RF barrier has been discussed. According to the values obtained for the *DR* parameter, the combination of a CW single carrier and a receiver formed by a heterodyne receiver and an envelope detector seems to be the best candidate, in terms of actual hardware prototype implementation and SAN nodes detection capacity.

Finally, we have tried the Kalman filter as an option to mitigate the multipath impairments for a SAN system, thus improving the node barrier detection accuracy. The use of a simple Kalman filter in the GMSK modulated signal case has provided an improvement of up to 3 m in the estimation of the position within the coverage area of the RF barrier.

We conclude that the system here presented constitutes a noteworthy alternative to classical WiFi-based tracking systems. It corrects some of the disadvantages existing in such systems and provides by-product features. The most relevant could be the chance to warrant privacy regarding the exchange of RFID information, the need of less reader nodes, and, last but not least, the resulting reduced level of power emissions.

The present network has been designed for a wooden items manufacturing chain. A SAN cell was deployed in strategic points wherein specific tasks were performed on each item. The time needed for the different tasks was variable. The SAN system helped to control the manufacturing chain speed, and at each process step, the item was perfectly tracked and remotely monitored. This contributed to improve the quality control, as well as the productivity.

Another likely application scenario would be given by a store using RFID tagged items, for both purposes of item tracking and stock update. The different movements of blocks of these items could be easily followed by placing them under SAN cells and making them to move along SAN spots to better tracking their positions. At present, this is solved by a network with multiple transceivers transmitting for the whole store and receiving answers from them. This situation produces a large interference and requires the deployment of multiple readers and repetitive questioning of the items to increase the reliability. Security, surveillance and health-care applications could be benefited of the use of the SAN systems.

At present, the research is ongoing, as each application scenario is individually analyzed according specific design issues. Other modulation schemes are under consideration, such as OFDM, choice that follows the case described in subsection 3.2. This case is easier and faster to implement due to the availability of chipsets in electronics market, even when it does not provide the most accurate operating features. The OFDM modulation option is expected to show a large improvement in the detection of the barrier limit, due to the shadow effect that largely affects the performance of this modulation scheme when the signal power level decreases under a specific value.

ACKNOWLEDGMENT

We would like to thank the support received from the People Program of 7th FrameWork Programme (2008 Marie Curie IOF Action).

REFERENCES

1. Liu, H.-Q. and H.-C. So, "Target tracking with line-of-sight identification in sensor networks under unknown measurement noises," *Progress In Electromagnetics Research*, Vol. 97, 373–389, 2009.
2. Liu, H.-Q., H.-C. So, K. W. K. Lui, and F. K. W. Chan, "Sensor selection for target tracking in sensor networks," *Progress In Electromagnetics Research*, Vol. 95, 267–282, 2009.
3. Kuo, S.-K., J.-Y. Hsu, and Y.-H. Hung, "Analysis and design of an UHF RFID metal tag using magnetic composite material as substrate," *Progress In Electromagnetics Research B*, Vol. 24, 49–62, 2010.
4. Loo, C.-H., A. Z. Elsherbeni, F. Yang, and D. Kajfez, "Experimental and simulation investigation of RFID blind spots," *Journal of Electromagnetic Waves and Applications*, Vol. 23, No. 5–6, 747–760, 2009.
5. Geok, T. K., A. W. Reza, and C.-P. Tan, "Objects tracking utilizing square grid RFID reader antenna network," *Journal of Electromagnetic Waves and Applications*, Vol. 22, No. 1, 27–38, 2008.
6. Lipsky, S. E., *Microwave Passive Direction Finding*, Wiley Interscience, 1987.
7. Poor, H., *An Introduction to Signal Detection and Estimation*, Ch. 4, New York, Springer-Verlag, 1985.
8. Liao, B., G. Liao, and J. Wen, "A method for DOA estimation in the presence of unknown non uniform noise," *Journal of Electromagnetic Waves and Applications*, Vol. 22, No. 14–15, 2113–2123, 2008.
9. Gomez, J., A. Tayebi, F. Saez de Adana, and O. Gutierrez, "Localization approach based on ray-tracing including the effect of human shadowing," *Progress In Electromagnetics Research Letters*, Vol. 15, 1–11, 2010.
10. Zhang, X., G. Feng, and D. Xu, "Blind direction of angle and time delay estimation algorithm for uniform linear array employing multi-invariance music," *Progress In Electromagnetics Research Letters*, Vol. 13, 11–20, 2010.

11. Rappaport, T. S., J. H. Reed, and B. D. Woerner, "Position location using wireless communications on highways of the future," *IEEE Communications Magazine*, Vol. 34, No. 10, 33–41, 1996.
12. Boukerche, A., H. A. B. Oliveira, E. F. Nakamura, and A. A. F. Loureiro, "Localization systems for wireless sensor networks," *IEEE Wireless Communications*, Vol. 14, No. 6, 6–12, 2007.
13. Benkic, K., M. Malajner, P. Planinšic, and Ž. Cucej, "Using RSSI value for distance estimation in wireless sensor networks based on ZigBee," *IEEE International Conference on Pervasive Computing and Communications*, 303–306, Galveston, Texas, USA, March 2009.
14. Zhao, J., Y. Zhang, and M. Ye, "Research on the received signal strength indication location algorithm for RFID system," *Proceedings of the International Symposium on Communications and Information Technologies*, 881–885, Bangkok, October 2006.
15. Kaemarungsi, K. and P. Krishnamurthy, "Properties of indoor received signal strength for WLAN location fingerprinting," *Proceedings of the MobiQuitous*, 14–23, Boston, Massachusetts, USA, August 22–26, 2004.
16. Kaemarungsi, K., "Distribution of WLAN received signal strength indication for indoor location determination," *IEEE International Symposium on Wireless Pervasive Computing*, 1–4, Phuket, Thailand, January 16–18, 2006.
17. Corbley, K. P., "WiFi inadequate as real-time asset and patient tracking solution," *Wireless Design Magazine*, 30–31, November 2008.
18. "Sensor area network for integrated systems health management," NASA SBIR contract NNX08CC91P, 2007.
19. Yu, G.-J., "An efficient storage policy for moving target path extraction in wireless sensor networks," *IET Communications*, Vol. 3, No. 9, 1488–1497, 2009.
20. Simon, D., *Optimal State Estimation: Kalman, H-infinity, and Nonlinear Approaches*, John Wiley & Sons, London, 2006.
21. Jiang, T., N. D. Sidiropoulos, and G. B. Giannakis, "Kalman filtering for power estimation in mobile communications," *IEEE Trans. Wireless Communications*, Vol. 2, No. 1, 151–161, 2003.
22. Ahson, S. A. and M. Ilyas, *RFID Handbook: Applications, Technology, Security, and Privacy*, 1st Edition, CRC Press, 2008.